

# ***K* x rays produced in collisions of bare ions with atoms: Contribution of multiple-electron transfer in Kr<sup>36+</sup>, Ar<sup>18+</sup>, and Ne<sup>10+</sup>+Ar collisions**

Hiro Tawara

*National Institute of Standards and Technology, Gaithersburg, Maryland 20899-8421, USA  
and Max Planck Institute for Nuclear Physics, D-69117 Heidelberg, Germany*

Endre Takács, Tibor Suta, and Károly Makónyi

*National Institute of Standards and Technology, Gaithersburg, Maryland 20899-8421, USA  
and University of Debrecen, Experimental Physics Department, Debrecen, Bem ter 18/A, H-4028, Hungary*

L. P. Ratliff and J. D. Gillaspay

*National Institute of Standards and Technology, Gaithersburg, Maryland 20899-8421, USA  
(Received 28 July 2005; revised manuscript received 5 October 2005; published 11 January 2006)*

*K* x rays have been observed in low energy collisions of bare Kr, Ar, and Ne ions with a neutral gas target. Although largely neglected previously, we have found that multiple-electron transfer processes play a significant role in shaping the x-ray spectra. The observed ratios of normal-satellite to hyper-satellite line intensities are found to be roughly independent of the ion species and much larger than those estimated from previously reported electron transfer cross sections, suggesting that there may be a strong correlation between two electrons during the electron transfer or during the subsequent cascades. It is suggested that exact knowledge of the initial and final principal and angular momentum quantum numbers ( $n, l$ ) in electron transfer are the most essential missing ingredients for understanding the entire x-ray emission process in astrophysical, laboratory, and technological plasmas.

DOI: [10.1103/PhysRevA.73.012704](https://doi.org/10.1103/PhysRevA.73.012704)

PACS number(s): 34.70.+e, 32.30.Rj, 32.70.Fw, 32.80.Cy

## I. INTRODUCTION

Recently, x-ray emission produced after electron transfer collisions of low energy, highly charged ions (HCI) with neutral atoms has captured great interest, particularly in applications to astrophysical observations of x rays from the tail of comets [1] and to laboratory as well as technological plasmas such as Tokamak fusion reactors [2]. Immediately after x-ray emission was reported from the tails of comets, fundamental laboratory investigations were performed [3–7] to measure x-ray intensities and spectral distributions at intermediate collision energies (a few keV/u), as models developed predicting that HCI interacting with the neutral particles in the comet tail were the source of these x rays (for a review, see Ref. [8]). X-ray spectra have also been observed at very low energies (around 10 eV/u) [9] and have been found to be significantly different when compared with those at intermediate energies. The observed x-ray spectra have been found to reflect the distributions of the states populated after electron transfer and in some single-electron transfer cases to be reproduced reasonably well with the initial ( $n_0l_0$ ) distributions calculated [10] using known atomic parameters [11,12].

So far, the majority of the investigations of these x rays have concentrated on those related to single-electron transfer processes. As the multiple-electron capture probabilities for HCI colliding with multielectron target atoms are known to be relatively high [13], it is natural to expect that some x rays formed through the multiple-electron transfer channels may be observed even in single collision conditions with thin gas targets. Therefore a detailed analysis of the measured x-ray

spectra requires information on both single and double (or more generally multiple-) electron capture processes. In the present experiments, x rays were produced and observed from bare ions, Kr<sup>36+</sup>, Ar<sup>18+</sup>, and Ne<sup>10+</sup>, in addition to H-like ions, Kr<sup>35+</sup>, Ar<sup>17+</sup>, and Ne<sup>9+</sup>. The collisions took place with neutral gas targets at the collision energy of  $\sim 4$  keV/u under single collision conditions.

## II. EXPERIMENT

The present experiments have been performed using ions from the NIST Electron Beam Ion Trap (EBIT) [14]. An electron beam with very high current density ( $>10^3$  A/cm<sup>2</sup>) interacts with the gas injected into the trap, thereby creating highly charged ions, which, upon extraction from the EBIT, have been used as projectiles in these studies. While there are many effects that determine the charge states created in the EBIT, as well as the charge state balance, different charge states can be produced by varying the electron beam energy. As a general operating procedure, the electron beam energy has to be set appropriately, reflecting the binding energies of the electrons to be removed. Because the creation of Kr<sup>36+</sup> ion beams is a noteworthy capability of the NIST EBIT, it is worthwhile to briefly mention how to obtain Kr<sup>36+</sup> ions with sufficient intensities for the present gas experiments: An electron beam with the energy of 28 keV and current of 150 mA was used to ionize the enriched <sup>86</sup>Kr gas. Optimal Kr<sup>36+</sup> production was obtained with an axial trapping time of  $\sim 1.5$  s. In these studies, it was found that cooling of the trapped Kr ions by injection of N<sub>2</sub> gas into the

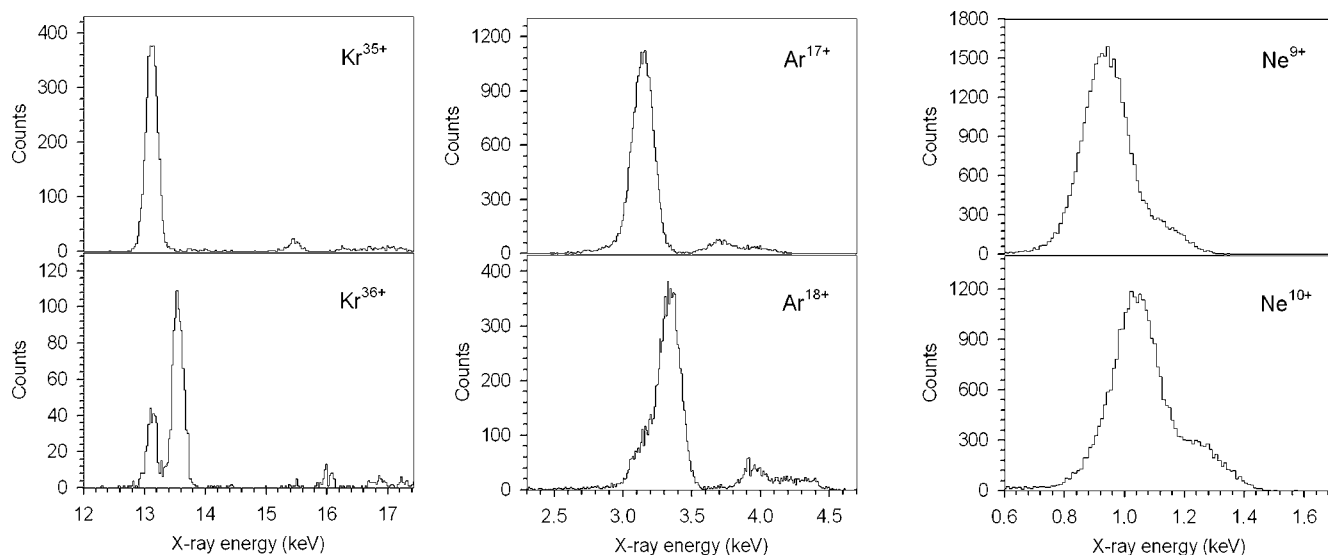


FIG. 1. Observed  $K$  x-ray spectra for  $\text{Kr}^{36+}$ ,  $\text{Ar}^{18+}$ ,  $\text{Ne}^{10+}$  (lower row) and  $\text{Kr}^{35+}$ ,  $\text{Ar}^{17+}$ ,  $\text{Ne}^{9+}$  (upper row) ions colliding with Ar gas target.

EBIT results in a significant increase (by a factor of about 5) in the intensity of extracted ions of  $\text{Kr}^{36+}$ . Ions were extracted from the EBIT at 8.25 kV per charge (approximately 4 keV/u), charge-state separated using an analyzing magnet, and sent into a gas target chamber [15]. A flux of approximately  $10^4$   $\text{Kr}^{36+}$  ions per second was directed through a collimation aperture and intersected a gas target produced from a single nozzle gas jet positioned at  $90^\circ$  with respect to the ion beam axis. Ar gas targets were used for the observations presented here, but additional measurements were also made with other gas targets (Ne,  $\text{O}_2$ ).

X rays produced in HCI collisions with gaseous targets were observed with a  $100 \text{ mm}^2$  Ge detector (with a  $0.4 \mu\text{m}$  polymer window in front of it), placed at  $90^\circ$  with respect to the incident ion beam axis. The window transmission has been accounted for in the present analysis. The detector was periodically energy-calibrated using various radioactive isotope sources. The energy resolution of the detector is roughly 130 eV for Ti  $K\alpha$  x rays at 4.50 keV. X-ray spectra have been observed as a function of the gas target pressure, to ensure that the observed x rays originate only from a single collision with the target gas atoms.

### III. RESULTS

Figure 1 shows typical observed x-ray spectra from  $\text{Kr}^{36+}$ ,  $\text{Kr}^{35+}$ ,  $\text{Ar}^{18+}$ ,  $\text{Ar}^{17+}$ ,  $\text{Ne}^{10+}$ , and  $\text{Ne}^{9+}$  ions colliding with an Ar gas target. The observed  $K$  x-ray spectra from H-like  $\text{Kr}^{35+}$ ,  $\text{Ar}^{17+}$ , and  $\text{Ne}^{9+}$  ( $1s$ ) ion-atom collisions (upper row in Fig. 1) are dominated by the normal-satellite  $K\alpha$  line ( $n=2 \rightarrow n=1$ ), which is peaked at 13.2, 3.1, and 0.95 keV, respectively. There are contributions from the  $K\beta$  ( $n=3 \rightarrow n=1$ ) and higher  $n$  transitions, including  $K\gamma$  ( $n=4 \rightarrow n=1$ ). It can be seen that each peak is quite symmetric around its maximum intensity, and that the  $K\beta$  line is well-separated from the  $K\alpha$  line (except for Ne ions, where they were not fully separated). The x-ray peaks in the upper row of Fig. 1 are

from  $K$  x rays which are emitted in part of the decay processes as the ion stabilizes into the ground state after a series of cascades, following the single-electron transfer into these H-like projectile ions. Note that, due to the limited energy resolution of the detector, x-ray satellite peaks from double-electron transfer into the  $(1s, nl, n'l')$  states cannot be resolved in these measurements.

In the lower row of Fig. 1, the dominant x-ray peaks are from  $K\alpha^h$  hyper-satellite transitions in bare ion-atom collisions.  $K\alpha^h$  hyper-satellite x rays are the result of decay of the excited  $2p$  states produced in single-electron transfer into the bare ions which have initially two vacancies in the  $K$  shell. The energies of the  $K\alpha^h$  x rays are shifted toward higher energy, compared to the normal-satellite,  $K\alpha$  since there is no screening effect (there is one electron already present in the  $K$  shell in the case of the normal-satellite  $K\alpha$  x ray). The x-ray energy of the peak on the low energy side of the main  $K\alpha^h$  peak has been found to match the normal-satellite  $K\alpha$  transition energy within the uncertainties of the present energy determination. This peak, which appears as a shoulder for Ar and Ne ions, but is a well-separated second peak for Kr ions (as can be seen in the lower row of Fig. 1), is attributed to the multiple electron transfer into these bare ions. The  $K\beta^h$  ( $\Delta n=2$ ) and  $K\gamma^h$  ( $\Delta n=3$ ) lines can also be seen in Fig. 1. The intensities of the  $K\beta^h$  and  $K\gamma^h$  lines are much lower than those of the  $K\alpha^h$  lines. It is also noted that the relative  $K\beta^h/K\alpha^h$ ,  $K\gamma^h/K\alpha^h$  and  $K\beta/K\alpha$ ,  $K\gamma/K\alpha$  intensity ratios are different for the various ions investigated.

Due to the limited energy resolution of the detector used in these experiments, fits to the data were done to analyze and separate the contribution of the normal-satellite line from strong hyper-satellite line for the observed x-ray spectrum for the  $\text{Ne}^{10+} + \text{Ar}$ , and  $\text{Ar}^{18+} + \text{Ar}$  data. In the  $\text{Kr}^{36+} + \text{Ar}$  spectrum the two lines are fully separated. Although we can distinguish the hyper-satellite from the satellite lines, the limited resolution prohibits us from distinguishing the various satellite lines from each other.

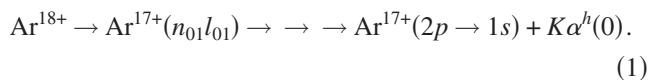
#### IV. DISCUSSION

In slow HCl-atom collisions, x-ray emissions occur after a series of cascade transitions because target electrons are usually transferred into high Rydberg states ( $n_0l_0$ ) of the incident ions [13] ( $n_0=5, 8,$  and  $14$  are expected for  $\text{Ne}^{10+}$ ,  $\text{Ar}^{18+}$ , and  $\text{Kr}^{36+} + \text{Ar}$  collisions, respectively [16]). The initial ( $n_0l_0$ ) distributions are critical in shaping the final x-ray spectrum through the cascade process [17,18]. Therefore, because the multiple-electron transfer cross sections become significant for heavy, highly charged ions [19,20], interpretation of x-ray spectra observed from such collisions requires the accurate knowledge of both single and multiple transfer processes.

We distinguish between the terms *transfer* and *capture* in that some of the electrons that are initially transferred do not remain captured because they are subsequently ejected from the ion during the cascade to the ground state (Auger emission). We use the notation  $\sigma_{j,i}$  to denote reaction cross sections for  $j$  electrons transferred and  $i$  electrons captured (kept). Our definition of the cross section thus includes the effect of a variable yield. To make the notation specific, we have chosen to discuss the case of  $\text{Ar}^{18+}$  ion-atom collisions. For simplification of the discussion, we use only the  $2p$  state as the final state before the emission of a  $K$  x-ray, and we consider only one- and two-electron transfer (we do not retain these simplifications in the full data analysis). The notation ( $\rightarrow\rightarrow\rightarrow$ ) represents a series of cascade processes.

##### A. Single-electron transfer ( $\sigma_{1,1}$ )

For bare ions, the important features of single-electron transfer processes, such as the initial ( $n_0l_0$ ) distributions, are reasonably well-understood, and x-ray emission processes are relatively simple:



The notation  $K\alpha^h(0)$  represents the emission of a  $K\alpha$  x ray in the presence of a spectator hole in the  $K$  shell (the superscript  $h$  for “hyper-satellite”) and zero (0) spectator electrons in higher ( $n>1$ ) shells. In this case, the x-ray energy is the highest among the possible  $K\alpha$  transitions.

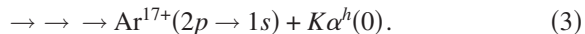
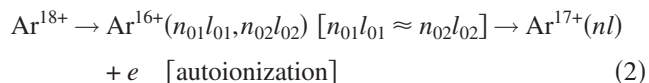
##### B. Double-electron transfer

Double-electron transfer can occur in two different ways, as described in the following two sections.

###### 1. Symmetric double-electron transfer ( $\sigma_{2,1}$ )

This process occurs when two electrons are transferred into states with similar quantum numbers ( $n_0l_0 \approx n_0l_0$ ), where the “0” indicates that the quantum number corresponds to the initial state into which the electron is captured, and the “1” or “2” indicates the first or second electron, respectively). These doubly excited states are stabilized mainly through autoionization processes, emitting one of the transferred electrons into the continuum. When the remaining electron cascades down to the  $2p$  shell, the emitted x-ray

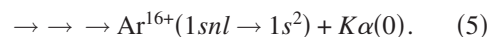
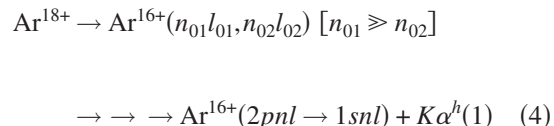
energy is the same as it would be from process (1).



###### 2. Asymmetric double-electron transfer ( $\sigma_{2,2}$ )

In this case, two electrons are transferred into asymmetric states, where one electron has a much smaller principal quantum number than the other ( $n_01 \gg n_02$ ). Such asymmetric distributions are formed through strong correlation between the two electrons during the transfer process [21]. The limited investigations done so far indicate that in this case the electron that is transferred into the higher excited state also goes preferentially into higher angular momentum states ( $l$ ), as expected for a statistical population distribution [19,22,23].

The doubly excited states formed in this case tend to be stabilized through radiative transitions, thus successively emitting two x rays with slightly different energies: first  $K\alpha^h(1)$  [e.g.,  $2pnl \rightarrow 1snl$  hyper-satellite line, with one electron in the ( $nl$ ) state], followed by  $K\alpha(0)$  ( $1snl \rightarrow 1s^2$ , with no spectator electron):



The energy of the  $K\alpha(0)$  transition is lower than that of the  $K\alpha^h(1)$  transition (see the center spectrum of the lower row in Fig. 1). Recent recoil ion coincidence experiments with *partially ionized* (but not bare)  $I^{q+}$  ( $q=10-25$ ) projectile ions have shown that, in most cases, Auger electron emission is far dominant over radiative emission [24,25].

##### C. Comparison to particle scattering experiments

A comparison of our direct measurement of x-ray line intensity ratios can be made with predictions inferred from previous measurements of the electron capture cross sections. It is clear from the discussion above that the hyper-satellite lines come from process (1) in single electron transfer, and processes (3) and (4) in double electron transfer, while the normal satellite lines originate only from process (5) in the double-electron transfer. Similar assignments can be extended to all the possible multiple electron transfer processes. A quantitative expression for the observed x-ray intensity ratio,  $R$ , between the normal satellite and hyper-satellite lines is related to the relevant electron capture cross sections as follows:

TABLE I. Comparison of the observed normal-to-hyper-satellite intensity ratios,  $I(K\alpha)/I(K\alpha^h)$  [Eq. (6)], and ratios estimated from the electron transferred cross sections measured with coincidence techniques [see Eq. (7)] for  $\text{Ne}^{10+}$ ,  $\text{Ar}^{18+}$ , and  $\text{Kr}^{36+}$  ions colliding with neutral Ar atom at 4 keV/u.

Ion	R(estimated)	R(observed)
$\text{Ne}^{10+}$	$0.10 \pm 0.02$	$0.29 \pm 0.03$
$\text{Ar}^{18+}$	$0.07 \pm 0.01$	$0.26 \pm 0.03$
$\text{Kr}^{36+}$		$0.30 \pm 0.03$

$$R = I(K\alpha)/I(K\alpha^h) \quad (6)$$

$$= \frac{A}{2} \left[ \frac{A}{2} + B \right] \quad (7)$$

with  $A$  denoting the sum of all cross sections for electron transfer reactions that result in the emission of a normal-satellite  $K\alpha$  x ray (i.e., those in which at *least two* electrons are kept on the ion after the relaxation to the ground state is complete),

$$\begin{aligned} A &= (\sigma_{2,2} + \sigma_{3,2} + \sigma_{4,2} + \sigma_{5,2} + \cdots) \\ &\quad + (\sigma_{3,3} + \sigma_{4,3} + \sigma_{5,3} + \sigma_{6,3} + \cdots) + \cdots \\ &= \sum_{j,i=2(j \geq i)}^{\infty} \sigma_{j,i} \end{aligned} \quad (8)$$

and  $B$  denotes the sum of all cross sections for electron transfer reactions that result in the emission of a hyper-satellite x ray (i.e., those in which at *most one* electron is kept on the ion after the relaxation to the ground state is complete),

$$B = \sigma_{1,1} + \sigma_{2,1} + \sigma_{3,1} + \sigma_{4,1} + \cdots = \sum_{j=1}^{\infty} \sigma_{j,1} \quad (9)$$

The factor of  $(1/2)$  needs to be included in Eq. (7) because only one of the two emitted x rays, either  $K\alpha$  or  $K\alpha^h$ , in a single event resulting from multiple-electron transfer is observed with the x-ray detector (small solid angle limit).

The values of  $R$  obtained directly from the present x-ray data (Fig. 1), after correction for window transmission and detector efficiencies, are compared with those estimated using Eq. (7) and the previously measured cross sections [25] in Table I. Two decimal point errors in the previous publication [25] have been corrected:  $\sigma_{4,3} = 0.09 \times 10^{-15} \text{ cm}^2$  and  $\sigma_{5,3} = 0.06 \times 10^{-15} \text{ cm}^2$ . Our values of  $R$  seem to be roughly independent of the ion, and significantly larger than those estimated from the previously measured cross sections (after propagating the approximately 20% uncertainties of the previous measurements).

We suspect that the main reason for the discrepancies between the ratios,  $R$ , that we directly observe and those indirectly estimated are due to the differences between the electron transfer processes for bare and partially ionized ions of the same charge but different atomic number. In bare ions such as  $\text{Ar}^{18+}$ , the electrons can in principle go into any principal quantum number ranging from  $n=1$  to infinity. In

partially ionized ions, however, the electrons which have not been stripped fill up some of the inner shells [up to  $nl=4p$  in  $\text{I}(18+)$ , for example], so additional electrons cannot be transferred to the filled levels. This reduction of available phase space in partially ionized ions will reduce the probabilities for transfer into the asymmetric states which have a higher fluorescence yield [see process (4)].

The initial  $l_0$  distributions after electron transfers are also critical in shaping the x-ray spectrum. Indeed the  $l_0$  distributions are known to be quite different for ions with different atomic number, even among those having the same ionic charge [26]. Such a difference in the initial  $l_0$  distributions can influence the transition probabilities and the branching ratios of the ions during cascades. To date, there is no detailed information, particularly on the initial  $(n_{01}l_{01}, n_{02}l_{02})$  distributions, for double-electron transfer in either bare or partially ionized ions. Thus it is important that future work be directed toward finding the correct cross sections and initial  $(n_{01}l_{01}, n_{02}l_{02})$  distributions in double-electron transfer for bare ions such as  $\text{Kr}^{36+}$  to compare with the direct x-ray measurements such as those presented here.

In addition to the issues discussed above, other possible contributing factors to the discrepancy shown in Table I include the effect of electron-electron correlation during the cascade (as opposed to during the transfer) and angular correlation and polarization effects.

## V. CONCLUSIONS

We have observed  $K$  x-ray spectra from low energy, bare  $\text{Kr}^{36+}$ ,  $\text{Ar}^{18+}$ , and  $\text{Ne}^{10+}$  ions colliding with Ar target atoms and found that, in addition to the expected hyper-satellite x-ray lines, we also see the so-called normal-satellite lines from He-like ions. We interpret this as direct spectroscopic evidence for multiple-electron transfer processes. Checks of the target gas pressure dependence confirmed that  $(1snl)$  states responsible for the normal-satellite lines are indeed being formed by multiple-electron transfer in single collisions of bare ions and not through successive single-electron transfer with multiple target atoms outside the main target region.

The relative brightness of the normal satellite lines is particularly striking in view of the fact that only a small fraction of all electron transfer events contribute to the formation of these lines. The large observed intensity can be explained by assuming that bare ions preferentially capture multiple electrons into initial asymmetric configurations with widely separated energies and thus enhanced fluorescence yields. This, in turn, makes it clear why it is not possible to predict the line ratios observed in bare ions using electron capture cross sections for partially ionized ions of the same charge.

We conclude, therefore, that multiple electron transfer processes play an important role in determining the x-ray spectra observed from low energy HCI-atom collisions, and we emphasize that precise knowledge of the initial electronic state distributions  $(n_{01}l_{01}, n_{02}l_{02}, \dots)$  after electron transfer is essential for the detailed analysis and interpretation of x-ray spectra measured from comets and other objects that involve charge exchange with highly charged ions.

## ACKNOWLEDGMENTS

The authors would like to thank Professor J. P. Briand for the loan of the gas jet target used in the present work, Professor V. P. Shevelko for a useful discussion on some theoretical aspects, C. J. Verzani for help in preparing this

manuscript, and H. Sakaue for providing the corrected values for  $\sigma_{4,3}$  and  $\sigma_{5,3}$ . E. T. was partially supported by the Hungarian Science Fund (OTKA T042729 and T046454). J.D.G. was partially supported by the U. S. Department of Energy, Office of Fusion Energy Sciences.

- 
- [1] C. M. Lisse, K. Dennerl, J. Englhauser, M. Hayden, F. E. Marshall, M. J. Mumma, R. Petre, P. Pye, M. J. Ricketts, J. Schmitt, J. Trümper, and R. G. West, *Science* **274**, 205 (1996); C. M. Lisse, D. J. Christian, K. Dennerl, K. J. Meech, R. Petre, H. A. Weaver, and S. J. Wolk, *ibid.* **292**, 1343 (2001).
- [2] H. Tawara, *The Physics of Multiply and Highly Charged Ions*, edited by F. J. Currell (Kluwer Academic, Dordrecht, 2003), Vol. 1, p. 103.
- [3] J. B. Greenwood, I. D. Williams, S. J. Smith, and A. Chutjian, *Astrophys. J.* **533**, L175 (2000).
- [4] H. Tawara, P. Richard, U. I. Safronova, A. A. Vasilyev, and M. Stöckli, *Can. J. Phys.* **80**, 821 (2002).
- [5] J. B. Greenwood, I. D. Williams, S. J. Smith, and A. Chutjian, *Phys. Rev. A* **63**, 062707 (2001).
- [6] H. Tawara, P. Richard, U. I. Safronova, A. A. Vasilyev, S. Hansen, and A. S. Shlyaptseva, *Phys. Rev. A* **65**, 042509 (2002).
- [7] A. A. Vasilyev, H. Tawara, P. Richard, and U. I. Safronova, *Can. J. Phys.* **80**, 65 (2002).
- [8] T. E. Cravens, *Science* **296**, 1042 (2002).
- [9] P. Beiersdorfer, C. M. Lisse, R. E. Olson, G. V. Brown, and H. Chen, *Astrophys. J.* **549**, L147 (2001).
- [10] J. A. Perez, R. E. Olson, and P. Beiersdorfer, *J. Phys. B* **34**, 3063 (2001).
- [11] V. Kharchenko and A. Dalgarno, *J. Geophys. Res.* **105**, 18351 (2000).
- [12] M. Rigazio, V. Kharchenko, and A. Dalgarno, *Phys. Rev. A* **66**, 064701 (2002).
- [13] R. K. Janev and H. P. Winter, *Phys. Rep.* **117**, 265 (1985).
- [14] J. D. Gillaspy, Y. Aglitskiy, E. W. Bell, C. M. Brown, C. T. Chantler, R. D. Deslattes, U. Feldman, L. T. Hudson, J. M. Laming, E. S. Meyer, C. A. Morgan, A. I. Pikin, J. R. Roberts, L. P. Ratliff, F. G. Serpa, J. Sugar, and E. Takacs, *Phys. Scr.*, T **59**, 392 (1995).
- [15] H. Tawara, E. Takács, L. P. Ratliff, J. D. Gillaspy, and K. Tőkési, *Nucl. Instrum. Methods Phys. Res. B* **205**, 605 (2003).
- [16] M. Kimura, N. Nakamura, H. Watanabe, I. Yamada, S. Ohtani, A. Danjo, A. Matsumoto, H. A. Sakaue, M. Sakurai, H. Tawara, and M. Yoshino, *J. Phys. B* **28**, L643 (1995).
- [17] P. Beiersdorfer, K. R. Boyce, G. V. Brown, H. Chen, S. M. Kahn, R. L. Kelley, M. May, R. E. Olson, F. S. Porter, C. K. Stahle, and W. A. Tillotson, *Science* **300**, 1558 (2003); P. Beiersdorfer, R. E. Olson, G. V. Brown, H. Chen, C. L. Harris, P. A. Neill, L. Schweikhard, S. B. Utter, and K. Widmann, *Phys. Rev. Lett.* **85**, 5090 (2000).
- [18] K. R. Cornelius, K. Wojtkowski, and R. E. Olson, *J. Phys. B* **33**, 2017 (2001).
- [19] M. Barat and P. Roncin, *J. Phys. B* **25**, 2205 (1992).
- [20] V. P. Shevelko and H. Tawara, *Atomic Multielectron Processes* (Springer-Verlag, Berlin, 1998).
- [21] N. Stolterfoht, K. Sommer, J. K. Swenson, C. C. Havener, and F. W. Meyer, *Phys. Rev. A* **42**, 5396 (1990).
- [22] J.-Y. Chesnel, H. Merabet, X. Husson, F. Fremont, D. Lecler, H. Jouin, C. Harel, and N. Stolterfoht, *Phys. Rev. A* **53**, 2337 (1996).
- [23] J.-Y. Chesnel, H. Merabet, B. Sulik, F. Fremont, C. Bedouet, X. Husson, M. Grether, and N. Stolterfoht, *Phys. Rev. A* **58**, 2935 (1998).
- [24] N. Selberg, C. Biedermann, and H. Cederquist, *Phys. Rev. A* **54**, 4127 (1996).
- [25] H. A. Sakaue, A. Danjo, K. Hosaka, D. Kato, M. Kimura, A. Matsumoto, N. Nakamura, S. Ohtani, M. Sakurai, H. Tawara, I. Yamada, and M. Yoshino, *J. Phys. B* **37**, 403 (2004).
- [26] H. Tawara and W. Fritsch, *Phys. Scr.*, T **28**, 58 (1989).